Bulgarian Chemical Communications, Volume 52, Special Issue F (pp. 47-53) 2020 *DOI: 10.34049/bcc.52.F.0008*

The influence of heat transfer on the energy efficiency in thin film evaporators

V. G. Rifert, P. A. Barabash, V. P. Boianivskyi*, V. V Sereda, A. S. Solomakha

National Technical University of Ukraine "Igor Sikorsky Kyiv Polytechnic Institute"

Received: July 26, 2020; Accepted: August 10, 2020

Today desalination of seawater provides world water production of 24.5 million m^3 per day. Some of the most common ways of desalinating are multi-effect distillation (MED) and multi-effect distillation with thermal (MED+TVC) and mechanical vapour compressors (MED+MVC). The key issues of this technology are the pollutant emissions into the atmosphere and the high energy consumption. A significant part of energy is consumed in evaporators, in which steam condenses in horizontal tubes at low pressures (from 7 to 50 kPa), and the evaporation of seawater occurs on the outer surface of the tubes. Such heat exchangers provide production of desalinated water from 0.5 to 500 m^3 per hour at a condensation temperature of water steam ranging from 40 to 80 ºC and are made of tubes with a diameter of 10 to 50 mm. The operating efficiency of the evaporators depends on the pressure loss (temperature difference between evaporation and condensation) and heat transfer in these devices. Heat transfer, in its turn, depends on the intensity of the evaporation processes in the falling film and the condensation inside the tubes. The present paper aims to analyse the effect of heat transfer during evaporation and condensation on the temperature difference and pressure loss in horizontal tube evaporators.

Keywords: desalination, evaporation, multi-effect distillation (MED), film condensation, heat transfer, thin film evaporator

INTRODUCTION

Thin film evaporators are widely used in desalination, food processing, petrochemical, and other fields because of their high heat transfer efficiency, small temperature difference, and small amount of liquid injection [1-4]. To reduce energy consumption in these systems, several methods are used: multi-effect distillation (MED), multi-effect distillation with thermal vapour compressor (MED+TVC) and multi-effect distillation with mechanical vapour compressor (MED+MVC).

Fig. 1 shows a principal scheme of a multi-effect MED [1]. Each effect consists of preheater, demister and thin film evaporator. The last effect is followed by the end condenser. Saturated steam with a temperature below 80^{o}C is fed to the evaporator of the first effect. Steam is the primary source of the thermal energy that drives the entire distillation process. At the outlet of the end condenser, seawater is divided into two streams: feedwater, which is fed to the first effect, passing through the preheater of each effect, and cooling seawater, which is discharged back into the sea. Preheating of sea water reduces the energy needs of the distillation process due to partial condensation of the total steam flow.

Feed water after preheating is sprayed on the tubular beam of the first effect, where it partially evaporates due to the heat released during condensation.

The unevaporated salt solution remains at the bottom of the effect and forms feed water for the next effect. The vapour produced, considered free of salts, passes through a demister in order to retain the brine droplets, and is directed to a preheater where part of it condenses. The rest of the steam is fed to the evaporator of the second effect at the lower pressure and temperature than in the first effect. In the second effect, the feed water, which is a salt solution, is subjected to an instantaneous evaporation process and forms additional steam. The distillate obtained from preheater and thin film evaporator is collected in a flash box. This process is repeated sequentially in each effect up to the last one.

In MED systems, the efficiency factor (COP) is almost proportional to the number of effects *n*. In MED+ MVC systems, the main energy costs consist of the isothermal operation of the centrifugal vapour compressor [5]:

$$W = \frac{\frac{k}{k-1} p_1 v_1 \left[\left(\frac{p_2}{p_1} \right)^{\frac{k-1}{k}} - 1 \right]}{\eta_c} = \frac{h_2 - h_1}{\eta_c}, \tag{1}$$

where W – compressor work, J/kg; p_1 – input compressor pressure, Pa; p_2 – output compressor pressure, Pa; v_1 – specific volume of steam at compressor inlet, m^3/kg; k – isentropic constant

* To whom all correspondence should be sent:
E-mail: volodya.81.vs@gmail.com

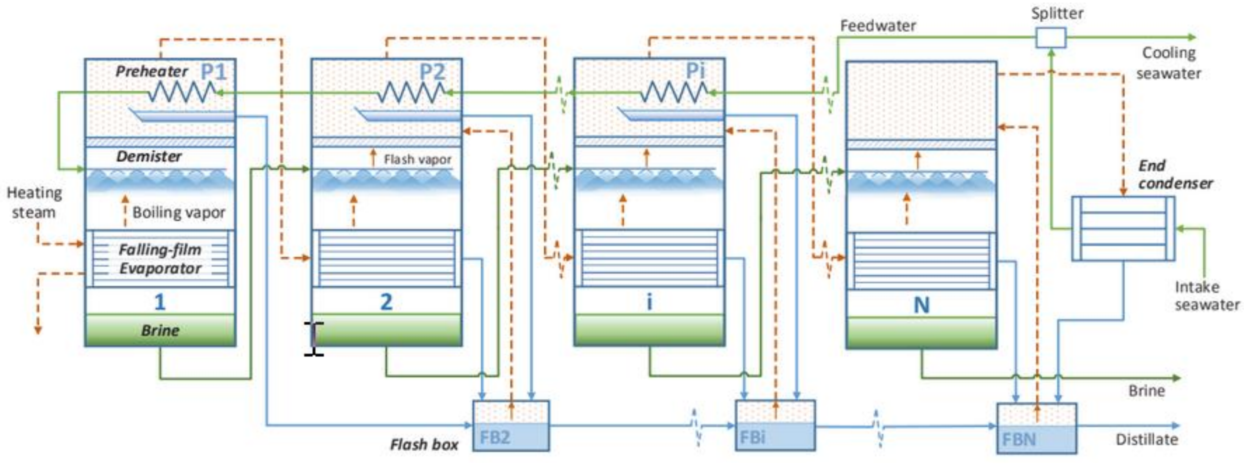

Fig. 1. Principal scheme of a multi-effect distillation system [1].

($k=C_p/C_v$=1.3 – for steam); h_2 – specific enthalpy of compressor exit, J/kg; h_1 – specific enthalpy of compressor inlet, J/kg; η_c – isentropic efficiency of compressor (η_c=0.85).

The energy losses of MED+TVC systems have been calculated assuming that it will have an overall thermal efficiency of 0.75, as suggested in [6]. The ejector efficiency can be expressed in terms of entrainment ratio by using the relationship:

$$\eta_e = (ER+1)\frac{h_4 - h_3}{h_1 - h_2}, \tag{2}$$

where ER – entrainment ratio, (kg/h vapour taken from evaporator and compressed by ejector) / (kg/h driving stream); h_1 – enthalpy of high pressure steam, J/kg;h_2 – enthalpy of steam after isentropic expansion in nozzle to pressure of entrained vapour, J/kg; h_3 – enthalpy of mixture at start of compression in diffuser section, J/kg; h_4 – enthalpy of mixture after isentropic compression to discharge pressure, J/kg.

Thus, the efficiency of all the 3 distillation systems (MED, MED+MVC and MED+TVC) depends on the number of effects and the pressure difference in the first effect p_1 and the last one p_n. For MED+TVC systems, the efficiency also depends on the pressure in the effect from which the steam enters the compressor.

The article analyses the factors influencing the pressure loss in the effects of the above-described installations and the overall pressure difference in the distillation systems. The methods for calculating heat transfer during evaporation in the falling film on the outer surface of horizontal tubes and during condensation inside these tubes are presented. The need to improve the methods of heat transfer calculation in thin film evaporators is substantiated.

FACTORS INFLUENCING PRESSURE LOSS

The hydraulic resistance in heat exchangers with convective two-phase processes involves pressure loss during heat transfer (during condensation or evaporation) and pressure loss in the connecting pipelines. Vacuum distillation also results in pressure loss due to non-condensing gases. In the process of concentration of heat-sensitive liquids, the temperature difference increases due to an increase in temperature depression caused by the pressure loss in the apparatus.

When designing multi-effect distillation of heat-sensitive liquids, it is necessary to know the permissible evaporation temperature to avoid precipitation when the solubility limit of any salt is reached. The lower temperature limit in a multi-effect distillation system is determined by the ambient temperature to allow condensation in the last effect of the installation.

With qualified design, the values of the above-described pressure losses and temperature differences in the distillation system can be minimized. Reducing pressure loss will reduce the temperature difference in one effect and, accordingly, increase the number of effects and energy efficiency of thin film evaporators.

Heat transfer components

Overall heat transfer coefficient (HTC) in thin film evaporators is determined by the formula:

$$U = \left(1/h_{con} + 1/h_{evap} + \delta_w / k_w + \sum_{i=1}^{n} R_i \right)^{-1} \tag{3}$$

where h_{con} – HTC during condensation of water vapour inside horizontal tubes with a diameter of 10 to 50 mm and a length of 1 to 16 m; h_{evap} – HTC upon evaporation of a film of liquid flowing down the rows of horizontal tubes. Large desalination plants can have more than 10 rows; δ_w, k_w – tube wall thickness and its thermal conductivity, respectively. In thermal desalination plants, δ_w = 0.5-2 mm and k_w = 60-100 W/(m·K). With these values, the thermal resistance of the tube wall can be neglected. In the absence of salt deposits and other contaminants on the surface of the tubes ($\sum_{i=1}^{n} R_i = 0$), the main thermal resistance in thin film evaporators can be calculated by the formula:

$$R = 1/h_{con} + 1/h_{evap} . \quad (4)$$

Heat transfer efficiencies during evaporation of a liquid film flowing down horizontal tubes

Calculation methods for HTCs during liquid evaporation on a smooth tube and on tubes with enhanced surface are given in [7-9]. Ribatski and Jacobi [7] analysed the studies of heat transfer during the evaporation of various liquids before 2005. The authors of [7] provided 16 formulae for calculating h_{evap}. In the thesis [8], analysis of 144 works was performed, 22 of which were published from 2005 to 2013. In addition to the formulae from [7], Bustamante [8] gave another 31 formulae for calculating h_{evap}.

Table 1 shows the formulae from [7, 8], which were obtained by evaporation of water vapour on a smooth tube. In these dependencies, the numerical values of the degrees under the criteria Re_f and Pr_l change from 0.06 to 0.85. Accordingly, the values of h_{evap} will be 1.5-10 times different.

Large discrepancies (more than three times) in the calculation of h_{evap} for various dependencies are also noted in [8, 9].

Rifert *et al.* [10-12] experimentally substantiated the model of heat transfer during evaporation and heating of a liquid film. This model is based on the analogy of the evaporation process with convective heat transfer at the initial thermal section of the development of velocity and temperature profiles in the laminar boundary layer [13].

Raising of the rate of average heat transfer with increasing mass flow rate noted by some investigators is caused by an increase in the initial thermal region length and by a decrease in the developing boundary layer thickness at all angular locations (φ coordinates) along the tube perimeter, but not by the transition to a turbulent regime at stable flow and heat transfer.

A comparison of $h_\varphi=f(\varphi)$ obtained for a gravity-falling film with that for a cross liquid flow shows that the heat transfer processes are analogous for both cases [14]. Hence, the experimentally determined values of the average HTCs in a liquid film were processed according to the system of dimensionless numbers accepted for heat transfer in a cross flow. The empirical dependence obtained:

$$Nu_{evap} = 0.295\,\mathrm{Re}_f^{0.63}\,\mathrm{Pr}_l^{0.36} \quad (5)$$

where $\mathrm{Re}_d = w_0 d/\nu_l$ (6)

w_0 – average film velocity, m/s

$$w_0 = (w_l^2 + 2gl_z)^{0.5} \quad (7)$$

l_z – distance between the tubes, м; w_l – film velocity during liquid separation:

$$w_l = 0.52(g\nu_l)^{0.33}\,\mathrm{Re}_f^{0.66} \;\; if \;\; \mathrm{Re}_f \le 220 \quad (8)$$

$$w_l = 1.55(g\nu_l)^{0.33}\,\mathrm{Re}_f^{0.462} \;\; if \;\; \mathrm{Re}_f > 220 \quad (9)$$

$$\mathrm{Re}_f = G/(\pi d \mu_l) . \quad (10)$$

Justification of Eqs. (8)-(10) is given in [15].

Equation 5 is almost the same as applied for calculation of heat transfer for cross flow over the in-line tube bundles and appropriately generalizes not only our test data, but also those of other investigators for film heating, cooling and evaporation [10]. In [11-12], it is proved that eq. (5) summarizes with sufficient accuracy (the discrepancy does not exceed 10%) the experimental data on heating and evaporation in a film of liquid flowing down horizontal tubes (single and in a bundle of tubes).

Heat transfer coefficients during condensation inside horizontal tubes

In thin film evaporators, condensation of heating steam occurs inside the tubes with a diameter from 10 to 50 mm and a length from 1 to 16 m. In MED systems, there can be from 2 to 10 effects. To prevent salt deposits, the steam temperature in the first effect should not exceed 80° C. The temperature in the last effect should not be lower than 30° C due to the limit for coolant temperature. Thus, the temperature difference in one effect can reach 3-10° C.

To determine h_{con}, a number of studies make use of dependencies given in Table 2. Calculations of h_{con} in different works give the values ranging from 4 kW/(m^2·K) to 15 kW/(m^2·K) [9]. If we take into account the possibility of heat transfer enhancement from evaporation by means of profiling tubes by 1.5-2 times [12, 14, 22, 24], then the values h_{evap} and h_{con} will be almost the same. The values h_{evap} and h_{con}, according to our calculations, will affect the value of overall heat transfer coefficient within 7-15%. It will lead to an increase in heat transfer area and capital costs (cost of tubes).

Table 1. Formulae for determining HTCs during liquid film evaporation

Study	Correlation	Study	Correlation
Mitrovic (1986) [16]	$Nu_{evap}=\frac{0.0137\,\mathrm{Re}_f^{0.349}\,\mathrm{Pr}_l^{0.5}(s/d)^{0.158}}{1+\exp(-0.0032\,\mathrm{Re}_f^{1.32})}$	Putilin *et al.* (1996) [22]	$Nu_{evap}=0.295\,\mathrm{Re}_f^{0.63}\,\mathrm{Pr}_l^{0.36}$
Rogers and Goindi (1989) [17]	$Nu_{evap}=0.063\,\mathrm{Re}_f^{0.466}\,Ar^{2/9}\,\mathrm{Pr}_l^{1/3}(\sin\theta/P(\theta))^{1/3}$	Liu and Zhu (2005) [23]	$Nu_{evap}=0.2116\,\mathrm{Re}_f^{0.29}\,\mathrm{Pr}_l^{0.515}\,Ar^{-0.39}$
Parken *et al.* (1990) [18]	$Nu_{evap}=0.042\,\mathrm{Re}_f^{0.15}\,\mathrm{Pr}_l^{0.53}$	Li *et al.* (2011a) [24]	$Nu_{evap}=7.426\,\mathrm{Re}_f^{-0.679}\,Bo^{-0.235}$
Rogers *et al.* (1995) [19]	$Nu_{evap}=0.2071\,\mathrm{Re}_f^{0.24}\,\mathrm{Pr}_l^{0.66}\,Ar^{-0.111}$	Li *et al.* (2011b) [25]	$Nu_{evap}=182.1\,\mathrm{Re}_f^{-1.56}$
Hu and Jacobi (1996) [21]	$Nu_{evap}=0.113\,\mathrm{Re}_f^{0.85}\,\mathrm{Pr}_l^{0.85}\,Ar^{-0.27}(s/d)^{0.04}$	Wang *et al.* (2013) [26]	$Nu_{evap}=1.57\,\mathrm{Re}_f^{0.49}\,\mathrm{Pr}_l^{0.4}\,Ar^{-0.23}(s/d)^{0.45}$
Nomenclature: *Ar* – Archimedes number; *Bo* – Bond number; *d* – outer diameter, m; Nu_{evap} – Nusselt number (= $h_{evap}d/k_l$); Pr_l – liquid Prandtl number; Re_f – film Reynolds number; s – tube spacing, m.			

Calculations of the process of condensation of water vapour inside the tubes with a diameter of 10 to 50 mm and a length of 1 to 16 m at t_s=40-90 ºC and heat flows from 15 to 40 kW/(m^2·K) demonstrate that at the tube inlet, the steam velocity can reach 100–150 m/s. Under such conditions, the steam velocity has a significant effect on heat transfer. On most surface of the tube, there will be an annular and intermediate (asymmetric) phase flow regime and the h_{con} values will differ from the HTCs in a stratified regime (see fig. 2).

The features of the film vapour condensation inside tubes (horizontal and vertical) are considered in reviews [30, 31], descriptions of new methods for calculating heat transfer during condensation are given in [34-38].

In [31-38], it is discussed that the area of condensation of the moving vapour in case of laminar condensate flow is not sufficiently studied experimentally, but this regime with Re_l<200 is characteristic of steam condensation in horizontal film evaporators.

EXPERIMENTAL RESEARCH

The detailed description of the experimental apparatus and method of heat transfer investigation during film condensation of moving vapour inside horizontal tube can be found in Rifert's previous publication [34]. The installation enables measuring circumferential local heat transfer coefficients by the "thickness wall" method. Using the "thickness wall" method allowed investigating the influence of the circumferential heat flux on the local values of the heat transfer coefficients. The research of water vapour condensation was performed at low pressures (ts = 46-70 ºC) in the middle of a smooth tube d = 18 mm with the following parameters: G = 3-52 kg/(m^{2}s), x = 0.94-0.1, q = 70-240 kW/m^2, Re_l=12-1500.

The flow pattern map of Rifert *et al*. [36, 37] was used to determine the limits of phase flow regimes. According to this regime map, the limits of the flow regimes are determined by the following dependencies:

at $\tau_f/\tau_g>10$ – annular flow (11)

at $1\le\tau_f/\tau_g\le10$ – intermediate flow (12)

at $\tau_f/\tau_g<1$ – stratified flow (13)

where values of the shear stress τ_f and the gravitational force τ_g are calculated in such a way:

$$\tau_f=C_f\rho_v w_v^2/2 \quad (14)$$

$$\tau_g=\rho_l g\delta. \quad (15)$$

Fig. 2 demonstrates the regime map for all the experimental data obtained. It shows that the data correspond to annular, intermediate and stratified phase flows.

Compare the experimental values of HTC with the calculations according to the formulae from Table 2. The results are shown in Fig. 3. It is obvious that the obtained experimental data significantly (more than 100%) diverge from the calculated data.

Fig. 4 shows a comparison of the overall HTC calculated by the formula (3) for different values of h_{con}. In this case, the values of h_{evap} for each option were calculated by the formula (5), while the values of h_{con} – by the formulae from Table 2.

The statistical comparison is summarized in Table 3. It contains the mean absolute deviation e_A, the average deviation e_R, and the standard deviation, σ_N, given in Eqs. (16)–(18), respectively, along with the percentage of predicted points lying within ± 10% error bars.

$$e_A = 1/n\sum 100\left|\left(h_{calc} - h_{exp}\right)/h_{exp}\right| \quad (16)$$

$$e_R = 1/n\sum 100\left[\left(h_{calc} - h_{exp}\right)/h_{exp}\right] \quad (17)$$

$$\sigma_N = \left[1/(n-1)\sum\left(e - e_R\right)^2\right]^{0.5} \quad (18)$$

where $e = 100\left[\left(h_{calc} - h_{exp}\right)/h_{exp}\right]$; n – number of calculation points. Fig. 4 and Table 3 show that the overall HTC values calculated using different formulae to determine h_{con} differ significantly. The calculation by the Nusselt formula appears to be the closest to the experimental data.

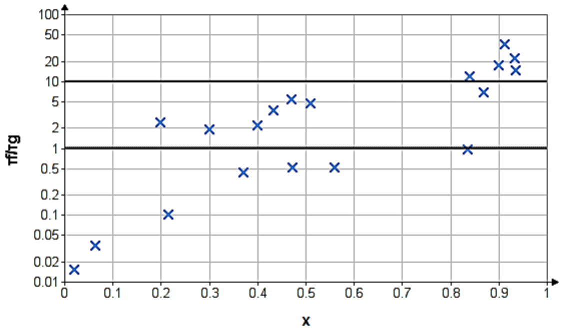

Fig. 2. Determining the phase flow regime

Table 2. Formulae for calculating HTCs in case of water vapour condensation

Authors, year	Heat transfer correlation
Nusselt [27] (1916)	$h_{con} = 0.728\left[\dfrac{k_l^3\rho_l\left(\rho_l - \rho_v\right)gh_{lv}}{\mu_l d\Delta T}\right]^{0.25}$
Boyko [28] (1966)	$h_{con} = 0.024\,\mathrm{Re}_l^{0.8}\,\mathrm{Pr}_l^{0.43}\left(1 + x\left(\rho_l/\rho_v - 1\right)\right)^{0.5}\lambda_l/d$
Traviss [29] (1998)	$h_{con} = Nu\lambda_l/d$, $Nu = F_{X.tt}\,\mathrm{Pr}_l\,\mathrm{Re}_l^{0.9}/F_2\;\; if\; F_{X.tt} \le 1;\;\; Nu = F_{X.tt}\,\mathrm{Pr}_l\,\mathrm{Re}_l^{0.9}/F_2\;\; if\; F_{X.tt} < 1$ *Equations for calculation of* $F_{X.tt}$ *and* F_2 *are given in* [29]
Shen [30] (2017)	$h_{con} = \theta h_{top} + \left(2\pi - \theta\right)h_{bot}$ $h_{bot} = 0.033\,\mathrm{Re}_l^{0.8}\,\mathrm{Pr}_l^{0.33}\left(k_l/d\right)\left[1 + \left(\dfrac{\rho_l}{\rho_v}\right)^{0.5}\left(\dfrac{x}{1-x}\right)\right]^{0.8}$, $h_{top} = \dfrac{0.02\,\mathrm{Re}_{vo}^{0.318}}{1 + 1.11X_{tt}^{0.755}}\left[\dfrac{\rho_l\left(\rho_l - \rho_v\right)gh_{lv}k_l^3}{d\mu_l\Delta T}\right]^{0.25}$

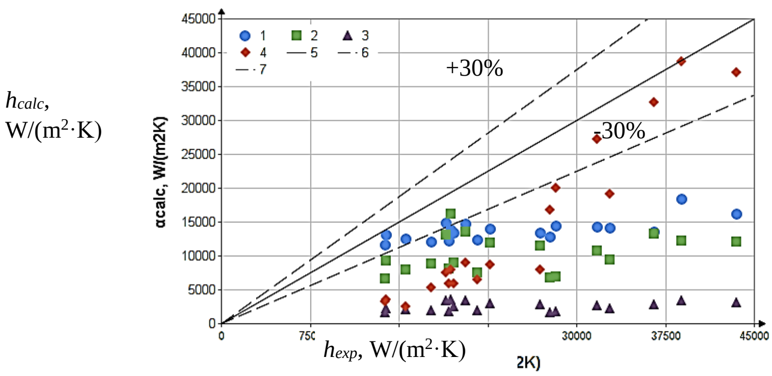

Fig. 3. Comparison of the obtained experimental data with correlations: 1 – Nusselt (1916) [27], 2 – Boyko (1966) [28], 3 – Shen (2017) [30], 4 – Traviss (1998) [29]

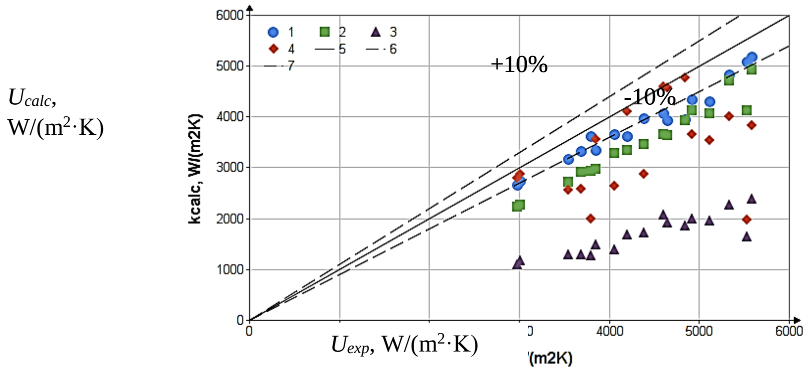

Fig. 4. Comparison of the overall HTC: 1 – Nusselt (1916) [27], 2 – Boyko (1966) [28], 3 – Shen (2017) [30], 4 – Traviss (1998) [29]

Table 3. Statistical comparison of the suggested method with the experimental data (in %)

Statistical comparison	e_A	e_R	σ_N	Percentage of predicted points lying within ±10% error bars
Nusselt [27]	10.8	-10.8	3.7	47
Boyko [28]	19.6	-19.6	5.0	5
Traviss [29]	24.6	-24.6	19.4	37
Shen [30]	62.1	-62.1	4.2	0

The studies of Rifert *et al*. [12, 14, 22] suggest various methods for heat transfer enhancement during liquid film evaporation. The analysis of these works leads to the conclusion that the most effective method of intensification in thin film evaporators is the longitudinal finning. This method allows increasing heat transfer by 60-80%, i.e. obtaining h_{evap} = 10-15 kW/(m^2 K). In this case, the accuracy of measuring the values of h_{con} according to the above calculation method will increase the heat transfer by 15-20%.

CONCLUSIONS

The actual values of HTCs during steam condensation at low pressure significantly differ from those calculated by the formulae of Nusselt [27], Boyko [28], Shen [30] and Traviss [29] (error more than 100%). The inaccuracy in determining h_{con} leads to a change in the values of the overall heat transfer coefficients in the range of 7-15%, and, accordingly, the surface area of heat transfer. The use of various methods of heat transfer enhancement during liquid film evaporation allows the increase of not only h_{evap}, but also of overall heat transfer coefficients by 15-20%. In carrying out further experimental studies, it is necessary to study the process of steam condensation in the conditions of steam velocity influence on heat transfer and at the regime parameters characteristic of thin film evaporators. Such research will allow improving thermal calculation of film evaporators and increasing their energy efficiency.

REFERENCES

1. B. Ortega-Delgado, L. García-Rodríguez, D.-C. Alarcón-Padilla, *Desalination and Water Treatment*, **97,** 94 (2017).
2. M. L. Elsayed, O. Mesalhy, R. H. Mohammed, L. C. Chow, *Appl. Therm. Eng*. **137,** 475 (2018).
3. P. Cyklis, *Applied Thermal Engineering*, **123,** 1365 (2017).
4. Q. Zhang, X. Zhang, C. Yin et al., *International Journal of Refrigeration*, **113,** 80 (2020).
5. M. R. Lubis, M. T. Holtzaple, *Aceb International Journal of Science and Technology*, **1** (1) 1 2012.
6. O. A. Hamed, A. M. Zamamiri, S. Aly, N. Lior, *Energy Conversion and Management*, **37**(4), 379 (1996).
7. G. Ribatski, A. M. Jacobi, *International Journal of Refrigeration*, **28,** 635 (2005).
8. J. G. Bustamante, Falling-film evaporation over horizontal rectangular tubes, PhD Thesis, School of Mechanical Engineering, Georgia, 2014, p. 254.
9. J. Uche, J. Artal, L. Serra, *Desalination*, **152,** 195 (2002).
10. V. G. Rifert, B. V. Andreev, Boiling and Condensation, Riga, 1981, p. 24.
11. V. G. Rifert, Yu. V. Putilin, V. L. Podbereznyi, *Journal of Engineering Physics*, **54**(5), 490 (1988).
12. V. G. Rifert, Yu. V. Putilin, V. L. Podberezny, *Journal of Enhanced Heat Transfer*, **8**(2), 91 (2001).
13. A. Zakauskas, V. Makaryavichus, A. Shlanchauskas, Heat transfer on the tubes band during cross liquid flow. Mintis., Vilnius, 1972.

14. Yu. V. Putilin, V. L. Podberezniy, V. G. Rifert, Proceedings of the 7th International Symposium on Fresh Water from the Sea, Amsterdam, vol. 1, 1980, p. 241.
15. V. Rifert, *Thermal Engineering*, **31**(11), 626. (1984).
16. J. Mitrovic, Eighth International Heat Transfer Conference, San Francisco, 1986, p. 1949.
17. J. T. Rogers, S. S. Goindi, *The Canadian Journal of Chemical Engineering*, **67,** 560 (1989).
18. W. H. Parken, L. S. Fletcher, V. Sernas et al., *J. Heat Transfer*, **112,** 744 (1990).
19. J. T. Rogers, S. S. G
20. oindi, M. Lamari, National Heat Transfer Conference, Portland, 1995, p. 3.
21. X. Hu, A. M Jacobi, *J. Heat Transfer*, **118,** 626 (1996b).
22. J. V. Putilin, V. L. Podberezny, V. G. Rifert, *Desalination*, **105**, 165 (1996).
23. Z.-H. Liu, Q.-Z. Zhu, *Chemical Engineering Communications*, **192**, 1334 (2005).
24. W. Li, X.-Y. Wu, Z. Luo et al., *Int. J. Heat Mass Transfer*, **54,** 2990 (2011a).
25. W. Li, X.-Y. Wu, Z. Luo et al., *Int. J. Heat Mass Transfer*, **54,** 1986 (2011b).
26. X. F. Wang, P. S. Hrnjak, S. Elbel, et al., *Journal of Heat Transfer*, **135**(7), 1 (2013).
27. W. Nusselt, *Zeitschrift VDI*, **60**, 541, 568 (1916).
28. L. D. Boyko, Heat Transfer in the Elements of Power Plants, (in Russian), 1966, p. 197.
29. D. P. Traviss, A. B. Baron, W. M. Rohsenow, Report No. DSR-72591-74, Massachusetts Institute of Technology, Cambridge, MA, 1971, p. 105.
30. S. Shen, Y. Wang, D. Yuan, *International Journal of Heat and Mass Transfer*, **114,** 816 (2017).
31. V. G. Rifert, V. V. Sereda, *Scientific journal "Thermal Science"*, **19**(5), 1769 (2015).
32. V. G. Rifert, V. V. Sereda, A.S. Solomakha, *Heat and Mass Transfer*, **55** (11), 3041 (2019).
33. Yu. E. Nikolaenko, E. S. Alekseik, D. V. Kozak, T. Yu. Nikolaienko, *Thermal Science and Engineering Progress*, **8**, 418 (2018).
34. V. G. Rifert, V. V. Sereda, P. A. Barabash, V. V. Gorin, *Thermal Science*, **21**(3), 1479 (2017).
35. V. G. Rifert, V. V. Sereda, P. A. Barabash et al., *Heat and Mass Transfer*. Vol. page (2020).
36. V. G. Rifert, V. V. Sereda, P. A. Barabash et al., *Energetika*, **64** (3), 146 (2018).
37. V. G. Rifert, V. V. Sereda, P. A. Barabash et al., *Bulg. Chem. Commun*., **50** (K), 58 (2018).
38. V. G. Rifert, V. V. Gorin, V. V. Sereda et al., *Journal of Engineering Physics and Thermophysics*, **92,** 797 (2019).